XY480 -EGU2011 -9048

EGU, General Assembly
Vienna Austria 03-08 April, 2011

S-wave identification by polarization filtering and waveform coherence analyses

Ortensia Amoroso (1), Nils Maercklin (1, 2) and Aldo Zollo (1)

(1) University of Naples Federico II, Naples, Italy (amoroso@na.infn.it), (2) AMRA S.c a r.l Via Nuova Agnano, Naples Italy

1. Motivation

High-resolution imaging with microseismic events requires the use of large and consistent data sets of seismic phase arrival times. In particular the S phase is important to derive physical parameters of the subsurface. Typically this phase is identified on one of the horizontal seismogram components by a change of signal amplitude and frequency as compared to the previous P phase. However, reliable S phase picking can be difficult for local events may because of a signal overlap with the P coda, the presence of converted phases, and possible S-wave splitting due to anisotropy. In this study we propose a new data processing technique aiming at uniquely identifing the S phase arrival using all available records from a seismic network. The technique combines polarization analysis of single three components (3C) recordings of an event with analysis of lateral waveform coherence across the network. This makes it possible to construct seismic sections in which the first arrival is the S-phase.

2. Method

The proposed method consists of four main steps. The first step is P-phase picking and event location, and the second one is the set-up of a polarization detector (Diehl *et al.*, 2009). We determine the direction L of the incoming P wave, compute the 3C covariance matrix (Montalbetti and Kanasewich, 1970), and rotate the observation system (ZNE) into the ray-coordinate system (LQT) (Plesinger *et al.*, 1986) to separate P from SV and SH energy. Then, we calculate the directivity D(t)

$$D(t) = \mathbf{L} \cdot \mathbf{e_{max}} \qquad (1)$$

where $\mathbf{e_{max}}$ is the eigenvector corresponding to the maximum eingenvalue of the covariance matrix, the rectilinearity P(t)

$$P(t) = \frac{(\lambda_1 - \lambda_2)^2 + (\lambda_1 - \lambda_3)^2 + (\lambda_2 - \lambda_3)^2}{2(\lambda_1 + \lambda_2 + \lambda_3)^2} \qquad (2)$$

where λ_i are the eingenvalues of the covariance matrix, and the ratio between transverse and total energy H(t)

$$H(t) = \frac{\sum_j (Q_j^2 + T_j^2)}{\sum_j (L_j^2 + Q_j^2 + T_j^2)} \qquad (3)$$

As an addition to the original method of Cichowicz (1993), we weight the function with the real amplitude of the transverse components. Our final characteristic function for S-wave detection CF_{SW} is

$$CF_{sw} = D^2 \cdot P^2 \cdot H^2 \cdot \sqrt{T^2 + Q^2} \qquad (4)$$

The third step deals with seismic section analyses. Once the CF_{SW} has been defined, the waveforms are collected in Common Receiver Gathers (CRG). If a single event is considered, the traces can be arranged in a Common Shot Gather lay-out (CSG). In case of large data sets of earthquakes from local or regional seismic networks, the number of sources is greater than the number of stations and the CRG layout is preferred. On each section we evaluate the lateral coherence of the S-phase through a linear move-out velocity analysis. In the fourth step an automatic picker is used.

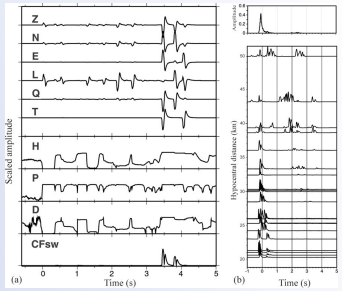

Figure 1. (a) **Synthetic seismogram example of 3C processing.** Z, N, E are the components in the observation system. L, Q, T are the rotated components. H, P, D are the polarization operators. (b) **CSG section of the CF_{SW}.** Each trace belongs to one simulated event recorded at a different station. The section was reduced considering $v_p \cdot (v_p/v_s - 1)^{-1} = 7\,km/s$. The top trace is the stack function. The time shift of 0.1 s is due to the finite length of the polarization filter.

3. Data and 3C analysis

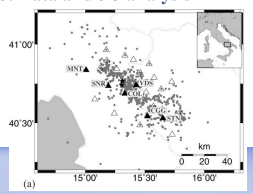

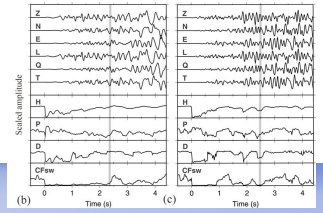

Figure 2. (a) **Map of seismicity of the area**. Gray dots represent the position of the earthquakes recorded by ISNet stations (white and black triangles).
(b) (c) **Example of 3C processing applied to two different local earthquakes recorded by station SNR**. The gray band indicates the theoretical S phase arrival time. In (b) we can see a good agreement with the theoretical S arrival and the simultaneous increase of H, D, P and CF_{SW}. In (c) we report a bad example: probably in this case the first maximum of the characteristic function corresponds to a converted phase.

The dataset consists of 5675 3C velocimeter records from 626 local earthquakes in the southern Apennines with ML (0.1, 3.3) and hypocentral distances D_{hypo} (2.3, 103.6 km), recorded by the ISNet network during the period 2007-2010. We selected traces with a signal to noise ratio greater than 5 and P pick accuracy better than 0.2 s, and we located the events with HYPO71 in a 1D velocity model. Each 3C seismogram was rotated from the laboratory reference system into the ray-coordinate system using the measured incidence angle and the backazimuth from the event location. Finally we computed the polarization operators and construct the CF_{SW} function.

4. S-phase sections

We arranged the CF_{SW} for each station in CRG. The seismic processing consisted in mean removal, amplitude balancing, envelope, and offset binning to improve the displayed distance range.
The sections (Fig. 3) show a high lateral coherence of the phase as a function of hypocentral distance. A clear 'first arrival' coincides with the arrival of the first S phase. This representation already provides an arrangement that can assist a manual picker in the detection of the S phase.
Linear move-out and amplitude stack velocity analysis supports the interpretation that the first arrival is an S phase travelling at a wave velocity of 2.5 to 3 km/s. These values are consistent with published velocity models for the Campano-Lucano Apennines (Maggi *et al.*, 2008; Matrullo *et al.*, 2011).

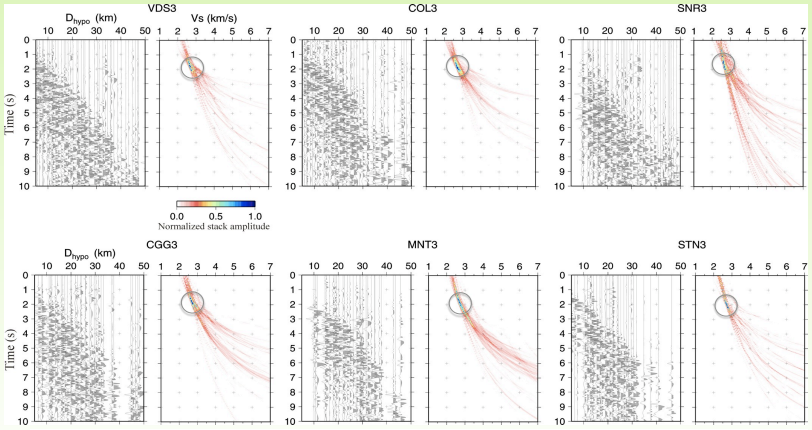

Figure 3. Common receiver gather sections and linear velocity analysis. For each station, the left panel shows the CF_{SW} section and the right panel the normalized stack amplitude for different velocity values. The location of the stack maximum indicates the best velocity (circle).

5. Picking

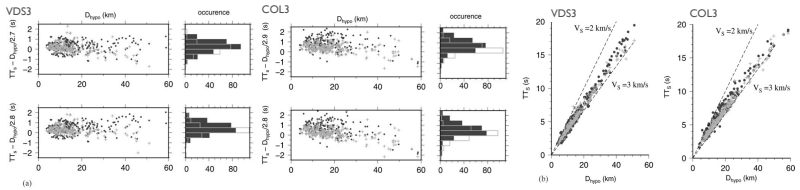

Figure 4. **Comparison between the manual readings on individual records and picking on the sections**. (a) The new readings (in dark gray dots) and manual readings (gray crosses) show the same distribution of residuals calculated considering two different homogeneous velocity models. (b) The travel-time vs hypocentral distance plot shows a greater number of readings for hypocentral distances greater than 30 km.

With the velocity obtained from the sections, a reference time for the S phase arrival can be computed. This time was used as a reference for an automatic autoregressive picker. Fig.4 shows the comparison between the manual readings of the S phase and automatic readings. The distributions of pick times in the reduced travel-time plots exhibit the same dispersion, but the automatic procedure provides about 40% more readings for each station.

6. Conclusions

We propose a technique for processing data to identify unambiguously the S arrival time using the three-component recordings from all stations of a seismic network. The proposed method supports the operator and can be used for both the analysis of individual events and for the massive semi-automatic analysis of large data sets.
The results presented in this study demonstrate the validity of the methodology for both routine practice and for more refined analysis. In fact, the sections allow the operator to replace manual picking of single traces with more efficient manual picking of sections, which is particularly suitable for large waveform data sets. To further improve the accuracy of the readings, refined re-picking techniques based on waveform similarity may be applied.

References

Cichowicz, A. (1993). An automatic S-phase picker, Bull. Seism. Soc. Am.,83,180-189.
Diehl T., N., Diechmann, E., Kissling and S., Husen (2009). Automatic S-wave picker for local earthquake tomography, Bull. Seism. Soc. Am., Vol. 99, No. 33, pp. 1906-1920, June 2009, doi:10.1785/0120080019.
Maggi C., Frepoli A., Cimini G.B., Console R., Chiappini M., (2008). Recent seismicity and crustal stress field in the Lucanian Apennines and surrounding areas (Southern Italy): Seismotectonic implications Tectonophysics, doi: 10.1016/j.tecto.2008.09.032 .
Matrullo E., Amoroso O., De Matteis R., C. Satriano and A. Zollo (2011). 1 D versus 3D velocity models for earthquake locations: a case study in Campania-Lucania region (Southern Italy), Geophysical Reasearch Abstract Vol. 13, EGU2011-9305, 2011.
Montalbetti J. F., and E. R. Kanasewich (1970). Enhancement of teleseismic body phases with a polarization filter. Geophysical Journal of the Royal Astronomical Society, 21(2), 119–129. doi:10.1111/j.1365- 246X.1970.tb01771.x. .
Plesinger, A., M., Hellweg and D., Seidel (1986). Interactive high resolution polarization analysis of boradband seismograms, J. Geophys. 59, 129-139.